Decomposition of crystalline ferromagnetic particles precipitated in amorphous paramagnetic Ni-P

1990 J. Phys.: Condens. Matter 2 2169

(http://iopscience.iop.org/0953-8984/2/9/006)

J. Phys.: Condens. Matter **2** (1990) 2169–2178. Printed in the UK

Decomposition of crystalline ferromagnetic particles precipitated in amorphous paramagnetic Ni–P

G Dietz and H D Schneider

II. Physikalisches Institut der Universität zu Köln, Zülpicher Strasse 77, D 5000 Köln 41, Federal Republic of Germany

Received 8 August 1989, in final form 18 October 1989

Abstract. According to small-angle x-ray scattering, amorphous Ni–P contains some volume per cent of metal-rich precipitations. During annealing, their diameters grow from about 2 nm in the as-prepared state to about 6 nm. It is shown by magnetic measurements that the inclusions are ferromagnetic single-domain particles embedded in a paramagnetic matrix. At sufficiently high temperatures such systems behave like superparamagnets. At 4.2 K, thermal agitation is too weak to flip the elementary magnetic moments. In this case, magnetisation curves can allow us to determine the coercivities and average saturation magnetisations. Annealing induces the two quantities measured at 4.2 K to change proportional to each other. This experimental fact justifies the application of a theory developed for fine non-interacting ferromagnetic particles having a magnetic shape anisotropy. The increase in the spontaneous magnetisation is attributed to the decomposition of the inclusions. With the aid of an approximation procedure the starting value of the phosphorus content and its decrease during annealing are estimated. These results and the values derived for the shape anisotropy agree well with those obtained through small-angle x-ray scattering. The starting phosphorus concentration of the precipitations proved to be independent of their volume fraction and the average composition of the samples. The observed kinetics fit in with the assumption of an activation energy spectrum. The lower limit starts at about 1.4 eV and is shifted on annealing to higher values.

1. Introduction

As-prepared electrodeposited Ni–P alloys are highly supersaturated microcrystalline and amorphous solid solutions of phosphorus in nickel. The defects represented by the phosphorus atoms distort the lattice increasingly as their concentration increases. Finally, at phosphorus concentrations above about 15 at.%, x-ray diffraction no longer indicates the existence of crystallites within the samples [1]. This does not mean that there is a sharp boundary between the crystalline and the amorphous phase at a well defined *average* phosphorus concentration x. According to x-ray diffraction patterns, material with 10 at.% $< x <$ 15 at.% is in a mixed state consisting of small crystallites embedded in an amorphous matrix. The metal concentration of the grains is some atomic per cent higher than that of the matrix. It seems that with regard to the *local* concentration the distinction between microcrystalline and amorphous is sharp. The number of grains per unit volume decreases with increasing x and even samples with $x >$ 15 at.% are not homogeneously amorphous but contain a few volume per cent of probably crystalline precipitations not visible by x-ray diffraction. This paper is concerned with the magnetic properties of these nickel-rich inclusions.

0953-8984/90/092169 + 10 $03.50

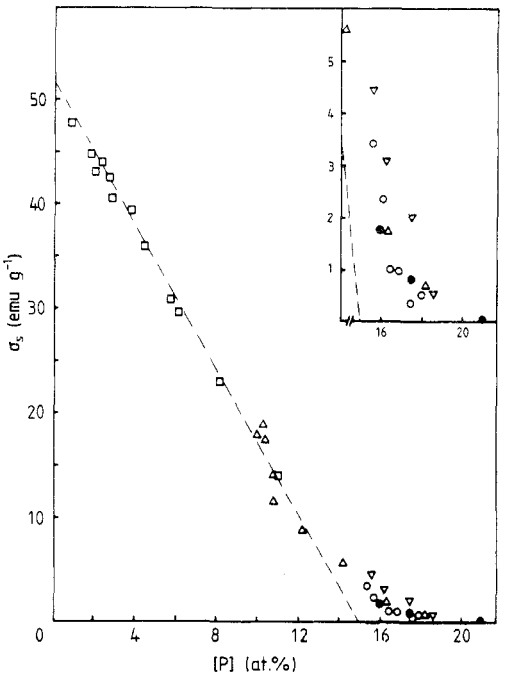

Figure 1. The composition dependence of the spontaneous magnetisation σ_s of as-prepared Ni–P alloys: □, [2]; ▽, [3]; △, [4]; ○, [5]; ●, this work. The inset demonstrates on an enlarged scale the effect of ferromagnetic inclusions precipitated in a non-ferromagnetic matrix.

Up to about 12.5 at.% P the saturation magnetisation of Ni–P decreases linearly with increasing phosphorus content and the extrapolated straight line cuts the concentration axis between 15 and 16 at.% P (figure 1). Homogeneously amorphous material containing more phosphorus is obviously non-ferromagnetic. Figure 1 shows the dependence of the specific saturation magnetisation at 4.2 K on the *average* phosphorus content. The positive deviations of the experimental results from the straight line must be attributed to crystalline ferromagnetic precipitations containing more nickel than the amorphous matrix.

This concept is supported by results obtained through small-angle x-ray scattering (SAXS) and transmission electron microscopy (TEM) [5–7]. SAXS diagrams and TEM micrographs taken from successively annealed samples indicate a kind of Ostwald ripening of the grains and a decrease in their phosphorus content. This result does not fit in with the concept in [8] where it was deduced from observations that the precipitations should be nearly pure nickel crystallites.

Extensive magnetic measurements were performed on three Ni–P samples having the same average compositions as those investigated with SAXS, namely 16, 17.5 and 21 at.% P. This paper reports on the results obtained at about 5 K in the as-deposited state and after stepwise annealing at 180 °C. Following theories developed in [9–11] for non-interacting single-domain ferromagnetic particles, the observations point to a decrease in the phosphorus content of the precipitated crystallites starting at about 12 at.% and ending at nearly pure nickel after annealing for some days. Obviously the microstructure of our samples differs from that of the samples investigated in [8].

2. Experimental details

The material was electrodeposited on well polished copper plates according to a recipe given in [12], applying a current density of 25 Å dm^2. The substrates were chemically

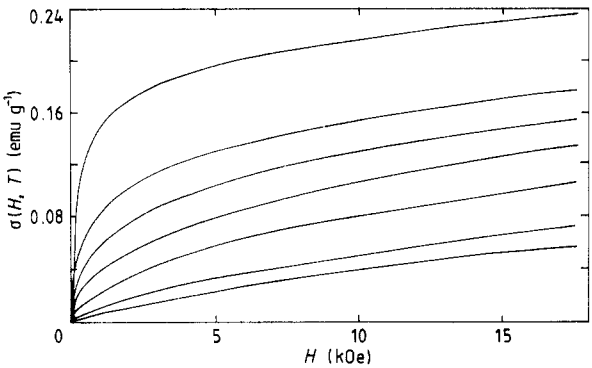

Figure 2. Magnetisation curves of $Ni_{79}P_{21}$ after annealing for 16 min at 180 °C taken at temperatures of 4.2 K, 50 K, 98 K, 152 K, 201 K, 252 K and 292 K (from top to bottom).

dissolved after preparation. The amorphous state of the samples was checked by x-ray diffraction. Their composition was determined by wet chemical analysis and by a magnetic method which demands that the material changes totally into its equilibrium phases—ferromagnetic Ni and paramagnetic Ni_3P—on annealing for some hours at 600 °C. This requirement was checked by x-ray diffraction and differential scanning calorimetry (DSC). The magnetisation curves of samples of well known masses (about 0.3 g) were taken between 4 and 300 K at seven selected temperatures in the as-prepared state and after each annealing step with the aid of a vibrating-sample magnetometer (VSM). The samples mounted in a Teflon cell were annealed in a preheated oil bath at 180 ± 2 °C for well defined periods of time. The changes in their magnetic properties during the heating period of some minutes were taken into account; those during quenching could be neglected. The annealing temperature was low enough to prevent crystallisation of the amorphous matrix even after 13 d at 180 °C. For annealing, the samples confined in their Teflon containers had to be removed from the VSM. The following remounting produced a possible error of about 4% in the specific saturation magnetisation σ_s. The detected signals were corrected with regard to contributions coming from the sample holder and the sample container and from magnetic image poles. The uncertainty in the coercivities H_c were about 10%.

3. Experimental results and discussion

As an example, figure 2 shows magnetisation curves obtained for $Ni_{79}P_{21}$ after annealing for 16 min at 180 °C. Their high-field parts can be represented by

$$\sigma = \sigma_s + \chi_{hf} H. \tag{1}$$

The first term comes from the particles which are ferromagnetic in the narrower sense. They are polarised parallel to the high external field H and below room temperature their contribution to the magnetisation σ_s is not noticeably increased by the applied field. Both the paramagnetic matrix and the superparamagnetic particles contribute to the second term in equation (1) including the field-independent high-field susceptibility χ_{hf}. These are particles with magnetic moments small enough to be switched by thermal agitation. σ_s can be determined by linear extrapolation of the high-field parts of the magnetisation curves (equation (1)).

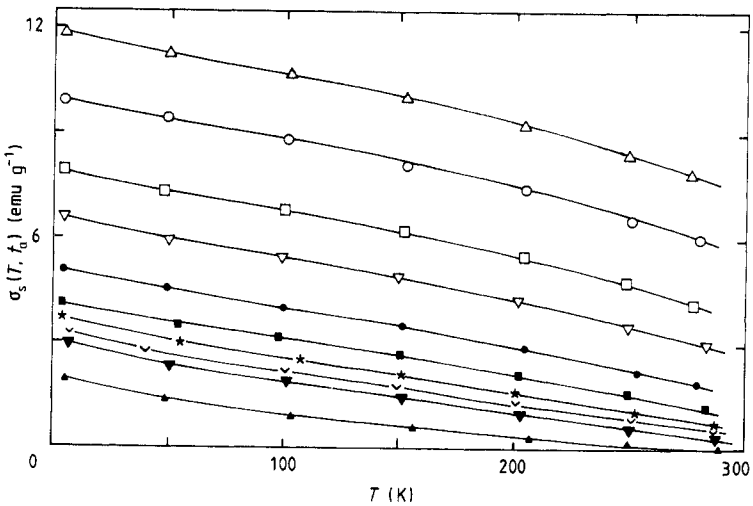

Figure 3. Spontaneous magnetisation σ_s versus temperature after annealing at 180 °C for various periods t_a: ▲, 0 min (as deposited); ▼, 4 min; ⋁, 8 min; ★, 16 min; ■, 32 min; ●, 64 min; ▽, 196 min; □, 580 min; ○, 3145 min; △, 18 440 min.

Figure 3 presents the temperature dependence of σ_s of $Ni_{84}P_{16}$ after annealing for certain periods of time at 180 °C. Apart from the magnitude of σ_s the curves obtained for the other samples are quite similar. The unusual curvature of the curves at low temperatures must be attributed to the fact that the first term in equation (1) is reduced with ascending temperature not only because of the decrease in the spontaneous magnetisation of the precipitated particles but also because more and more particles become superparamagnetic as soon as their blocking temperature is exceeded [13, 14]. The superparamagnetic contribution is significant even at 50 K and is pronounced at higher temperatures. In this region, H_c and the remanent magnetisation σ_r are smaller than the experimental error. The complicated superparamagnetic behaviour will be treated in a subsequent paper. This paper is restricted to the magnetic properties of the samples at about 4 K and their change with low-temperature annealing.

First we have to look for the single-domain properties of the precipitated particles. According to SAXS, they have average diameters between 2 and 3 nm in the as-plated samples and between 5 and 6 nm after long-time annealing at about 200 °C [6]. Taking into account the relatively small saturation magnetisation of ferromagnetic Ni–P alloys (figure 1), these values are well below the critical diameters of single-domain particles estimated with the aid of known models [15]. The particles are also small enough that rotation in unison is the favoured mechanism of magnetisation reversal [16]. As the volume fraction occupied by the particles proved to be below 15% [6], their magnetic interaction can be neglected. This conclusion is supported by the values of the coercivity H_c measured at about 5 K. The H_c-values of the three samples agree within the experimental error before and after annealing although the volume fractions occupied by the precipitations differ by a factor of 10. In systems with interacting particles, H_c would be smaller, the higher their concentration.

Additionally, we can assume that the blocking temperatures of the ferromagnetic particles are appreciably higher than 5 K because the high-field susceptibilities χ_{hf} of the samples are as small as the paramagnetic susceptibility of conduction electrons (table 1). They decrease as the phosphorus concentration increases, probably owing to a

Table 1. Properties of the as-prepared Ni–P samples: x, average phosphorus content; χ_{hf}, high-field susceptibility at 4.2 K; ρ, average density; m_f/m, mass fraction of the ferromagnetic inclusions; $\rho_0 = \rho_f(t = 0)$, density of ferromagnetic inclusions; $p_0 = p_f$ $(t = 0)$, phosphorus content of ferromagnetic inclusions.

x (at.% P)	χ_{hf} (10^{-6} cm^3 g^{-1})	m_f/m	ρ (g cm^{-3})	ρ_0 (g cm^{-3})	p_0
16	9	0.17	8.12	8.17	0.122
17.5	6	0.11	8.06	8.15	0.130
21	3	0.011	7.93	8.15	0.129

lower carrier density, and increase by some per cent on annealing. If there were some superparamagnetic particles at 5 K, χ_{hf} should be larger and should decrease on annealing because the magnetic moment of the particles would be enlarged and also their blocking temperature. As a consequence the number of superparamagnetic particles and their contribution to the high-field susceptibility should decrease.

Summarising, our samples are systems of non-interacting ferromagnetic single-domain particles embedded in a paramagnetic matrix. Their magnetic moments are too large to be switched by thermal agitation around 5 K. Under the action of an external field they are reversed by homogeneous rotation. These conditions are sufficient to apply theories developed in [9, 10, 13, 16] for this case.

Provided that the particles can be represented by ellipsoids of revolution with average axes a and b and corresponding demagnetising factors N_a and N_b, the models have a linear correlation between the coercivity H_c and the spontaneous magnetisation I_s (magnetisation per unit volume) of the particles:

$$H_c = g(N_b - N_a)I_s. \tag{2}$$

$g = 0.479$ in the case of random orientation of the particle axes. $g = 1$ if the long axes of the ellipsoids are all parallel to the magnetising field. I_s is the magnetisation (magnetic moment per unit volume) of the particles. If magnetocrystalline anisotropy dominates (anisotropy constant K), the theory yields

$$H_c = 2g(K/I_s). \tag{3}$$

This investigation showed that both H_c and the specific magnetisation σ_s of the samples at 5 K *increased* on isothermal annealing at 180 °C and that during the first 30–50 h resulted in a linear correlation (figure 4). It is impossible to fit a superposed term proportional to σ_s^{-1} to the experimental data. Therefore in the following we shall discuss our observations on the basis of equation (2). This will lead to reasonable results which agree well with those obtained with other methods. We assume that $g \simeq 0.5$. SAXS revealed a certain preferred orientation of the long axes a of the particles normal to the plane of the samples but the external field was applied in plane and there the axes are randomly oriented.

As a first step we have to relate the magnetisation I_s of the grains with the measured specific magnetisation σ_s of the samples. The specific magnetisation σ_f of the grains is

$$\sigma_f = (m/m_f)\sigma_s = (V\rho/V_f\rho_f)\sigma_s \tag{4}$$

where m_f, V_f and ρ_f are the mass, the volume and the density of the ferromagnetic component whereas the corresponding magnitudes without indices describe the properties of the total sample. Replacing $I_s = \sigma_f\rho_f$, one obtains

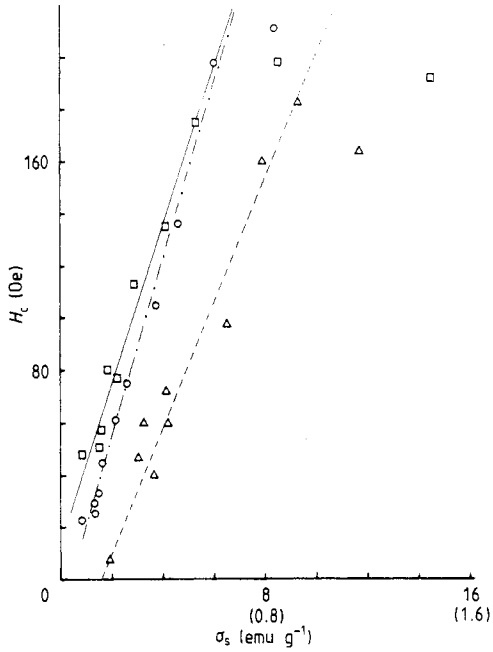

Figure 4. During the first 30–50 h of annealing the coercivity H_c of the samples at 4.2 K grew linearly with the accompanying saturation magnetisation σ_s: △, 16 at.% P; ○, 17.5 at.% P. The scale in parentheses is valid for the experimental results (□) obtained with the sample containing 21 at.% P.

$$I_s = (V/V_f)\rho\sigma_s \tag{5}$$

and ends up with

$$H_c = g(N_b - N_a)(V/V_f)\rho\sigma_s \text{ Oe}. \tag{6}$$

Equation (7) presents a linear relation between H_c and σ_s according to figure 4 and tells us that $(N_b - N_a)/V_f$ is not affected by annealing. It is possible that, during progressive decomposition of the material, V_f increases, but it is improbable that $N_b - N_a$ decreases exactly to such an extent that the ratio remains constant. Instead of this it is reasonable to assume that both quantities, $N_b - N_a$ and V_f, remain constant during the first 50 h of annealing. This agrees with conclusions drawn from SAXS and TEM [6, 7].

Annealing for longer than 60 h induces deviations in H_c from the initially linear run. Obviously the preconditions of the theory are not obeyed. Probably V_f increases now or the particles become so large that magnetisation no longer reverses by homogeneous rotation or that magnetic interactions come into play. Each of these effects reduces H_c.

If V/V_f does not change during annealing, the increase in σ_s must be attributed to the decrease in the phosphorus content of the ferromagnetic grains. In a stepwise approximation the data summarised in figure 4 will be used to estimate the gradual decomposition. It is plain that we shall end up with only average data. According to our approximate consideration, it is justified to assume that at the end of the thermal treatment the particles consist of pure nickel having a magnetisation $\sigma_0 = 57.5$ emu g^{-1}. Then $m_f/m = \sigma_{se}/\sigma_f$, where σ_{se} is the finally measured total magnetisation of the sample. The corresponding values of m_f/m in table 1 agree fairly well with those derived from SAXS for samples of the same composition [6, 7]. The densities ρ of the samples in table 1 were determined with a buoyancy technique. With the density ρ_{Ni} of nickel (8.9 g cm^{-3}),

$$V/V_f = m\rho_{Ni}/m_f\rho. \tag{7}$$

As explained above, this quantity is initially not affected by annealing. At this stage of

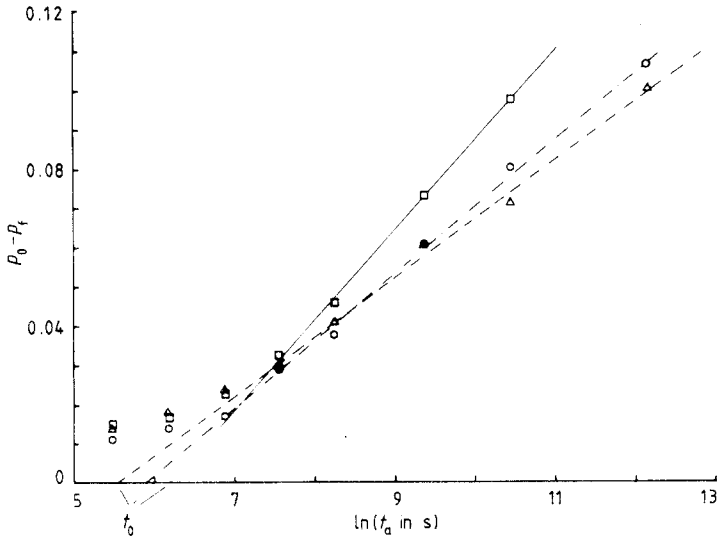

Figure 5. The shift $p_0 - p_f$ of the phosphorus content with increasing annealing time t_a for the following *average* phosphorus contents: △, 16 at.% P; ○, 17 at.% P; □, 21 at.% P. The fictitious times t_0 result from an extrapolation of the linear parts of the curves.

the procedure it is unknown but it does not dramatically deviate from m/m_f. So as a first step we calculate the magnetisation σ_f of the particles from

$$\sigma_f = (m/m_f)\sigma_s \simeq (V/V_f)\sigma_s. \tag{8}$$

According to a least-squares fit of many experimental data the relation between the specific magnetisation σ and the phosphorus concentration p of Ni–P alloys is represented by

$$\sigma = -383p + 57.5 \text{ emu g}^{-1} \qquad (p < 0.15). \tag{9}$$

Identifying σ in equation (9) with σ_f in equation (8), we obtain an approximate phosphorus concentration p_f of the grains in each annealing state. With these values we calculate the density ρ_f of the ferromagnetic component using empirical formulae basing on nearly 100 experimental data obtained for $Ni_{1-p}P_p$:

$$\rho = -3p + 8.54 \text{ g cm}^{-3} \qquad \text{for } 0.1 < p < 0.25 \tag{10}$$

$$\rho = -6.6p + 8.9 \text{ g cm}^{-3} \qquad \text{for } 0 < p < 0.1. \tag{11}$$

Now we have corrected values for

$$m/m_f = (\rho/\rho_f)(V/V_f). \tag{12}$$

Repeating the procedure just described with these new values, we find corrected p_f- and ρ_f-values. After at most three steps of this kind the calculated values remain constant. The results for the samples in the as-prepared state are inserted into table 1; the others are included in figure 5 in a semilogarithmic presentation. Within the accuracy of our estimation the ferromagnetic precipitations start with identical phosphorus concentrations p_0 independent of their volume fraction and the average concentration of the samples. According to remarks in section 1, $p_0 \simeq 0.13$ means that the ferromagnetic precipitations are crystalline. The three samples behave similarly during the first 10–15 min of annealing at 180 °C. Thereafter the grains decompose more rapidly, the smaller

Table 2. Some additional results of the analysis of the experimental data: q, factor of proportionality in equation (13); τ_1, lower limit of the relaxation time spectrum at 180 °C; Q_1, lower limit of the activation energy spectrum; N_a, demagnetising factor along the long axis of the small particles (assumed as ellipsoids of revolution); N_b, demagnetising factor along the short axis; a/b, ratio of the axes.

x (at.% P)	q	τ_1 (s)	Q_1 (eV)	$N_a - N_b$	N_a	N_b	a/b
16	1.6	470	1.43	1.13	1.34	2.47	1.21
17.5	1.7	650	1.44	1.01	1.42	2.43	1.17
21	2.2	880	1.45	0.9	1.49	2.39	1.14

their volume fraction. At least after about 15 min the experimental data $p_0 - p_f$ increase linearly with increasing logarithm of the annealing time t_a or, in other words,

$$d(p_0 - p_f)/dt_a = q/t_a. \tag{13}$$

Table 2 includes the values q resulting from a linear fit. Analysing SAXS data, we find that $q \simeq 2.1$. In view of the lower accuracy of the SAXS measurements the agreement is satisfying.

The rates described by equation (13) correspond to a process not following first-order kinetics. On the assumption that the activation energy for the diffusion is a function of the variable $p_f(t_a)$ during isothermal annealing (see, e.g., [17]), the rate equation (13) can be written as

$$dp_f/dt_a = -q \exp[-(E_0 - np)/k_B T]. \tag{14}$$

Integration of equation (15) leads to a logarithmic time relation according to the observation

$$p_0 - p_f(t_a) = u + v \ln t_a. \tag{15}$$

It is impossible to derive the three parameters E_0, q and n in equation (14) from empirical curves as represented by equation (15). Equation (14) means that the effective activation energy $E_0 - np$ increases as p_f decreases. This picture is equivalent to the assumption of an energy spectrum as is usual in the case of irreversible relaxation in amorphous material [18]. On the assumption of a box-like distribution of the relaxation times τ over $\ln \tau$ with τ_1 as the lower and τ_2 as the upper limit, the relaxation function $r(t)$ which describes the time dependence of the relaxing physical property is given by [19]

$$r(t) \simeq 1 + [\ln(\tau_2/\tau_1)]^{-1}[C - \ln(t/\tau_2)] \tag{16}$$

in a time interval $\tau_1 \ll t \ll \tau_2$. $C = 0.577\,216\ldots$ is Euler's number. The extrapolation of equation (16) to $r(t) = 0$ yields a fictitious temperature $t_0 = \tau_1/e^C$. In this way the lower limit of the relaxation time spectrum can be determined. In our case, $p_0 - p(t_a)$ is the relaxing quantity (figure 5). The resulting τ_1-values listed in table 2 increase as the volume fraction of the crystalline inclusions decrease.

Further analysis requires isothermal annealing of other identical samples at other temperatures. This ought to be done at sufficiently low temperatures T_a that crystallisation of the amorphous matrix does not start even after long-time annealing. This means that $T_a < 200$ °C. On the other hand the annealing time to induce a certain change grows exponentially as the temperature is lowered. So the range of practicable annealing temperatures is very small and we had to be content with only one annealing temperature.

As a consequence, further interpretation is not possible without some additional assumptions. Provided that τ_1 follows an Arrhenius law

$$\tau_1 = \tau_\infty \exp(Q_1/k_B T) \tag{17}$$

and $\tau_\infty^{-1} \simeq 10^{13}$, the lower limit Q_1 of the activation energies corresponding to the measured τ_1 result in the values listed in table 2. They agree for the three samples, indicating that the elementary diffusion process responsible for the decomposition of the precipitations is the same. Furthermore the values are of the order of magnitude observed for the diffusion of phosphorus in 3d transition metals. This rough estimation must not be overrated. It only demonstrates that the results fit in with the proposed model also in this respect.

The consistency of the results supports the applied model. So we should be able to draw additional information from equation (6). Neglecting the last two annealing steps, we found a factor of proportionality c between H_c and σ_s independent of thermal treatment and showed that the assumption V/V_f = constant leads to reasonable conclusions. The average densities ρ of the samples and

$$c = g(N_b - N_a)\rho(V/V_f) \tag{18}$$

are measured quantities. So we are able to calculate $N_b - N_a$ (table 2). Taking into account that $2N_b + N_a = 2\pi$ for ellipsoids of revolution and $g \simeq 0.5$, we obtain the average values for N_a and N_b listed in table 2. The relation between $N_b - N_a$ and the ratio of the axes of the ellipsoids is known (see, e.g., [17]). The results for our samples are summarised in the last column of table 2. They tell us that the precipitated particles are somewhat elongated, to the same extent as has been derived from SAXS. Corresponding results obtained for Fe–P, Co–P and Ni–P will be published in a subsequent paper. This agreement is additional support for the above-assumed concept.

4. Conclusions

SAXS and TEM performed on electrodeposited amorphous Ni–P alloys showed that the material contains some volume per cent of small precipitations having a lower phosphorus concentration than the matrix. Owing to annealing, their mean diameter and their metal concentration increase whereas the volume fraction that they occupy remains nearly constant. This means that the larger grains grow at the expense of the smaller grains. According to magnetic measurements the samples include ferromagnetic particles embedded in the amorphous paramagnetic matrix. Above around 70 K they behave at least partly as superparamagnets. This paper is concerned with their properties at about 5 K well below any blocking temperature.

It turned out that, as a result of annealing, the coercivity H_c of the samples alters proportionally to their saturation magnetisation σ_s. This relation is predicted for small non-interacting single-domain particles having magnetic shape anisotropy. Our samples meet the first two preconditions. On the assumption that the third condition holds too, we can attribute the observed increase in the magnetisation to the increase in the metal concentration within the grains. An approximation procedure allows us to estimate the gradual decomposition during thermal treatment. Despite the different average compositions of the samples and the widely differing volume fractions of their ferromagnetic components, the results support the assumed model in several respects. The quantitative results are at least of the correct order of magnitude and conform with those

obtained through other techniques. This means that, during the first hours of annealing, the nucleation of additional ferromagnetic grains is unimportant. It may well be that, during long-time annealing, this process contributes to the deviations of the $H_c(\sigma_s)$-relations from linear runs.

This investigation has identified the inhomogeneities detected for the first time with SAXS [6] as small ferromagnetic crystalline precipitations of reduced phosphorus content. Because of the small volume fraction occupied by the grains the change in the average composition of the matrix due to diffusion of phosphorus is negligible. Large-angle x-ray diffraction yields patterns characteristic for amorphous material even after annealing at 180 °C for nearly 2 weeks. Therefore we attribute the observed effects to changes within grains which have formed during electrodeposition.

Acknowledgments

The authors acknowledge gratefully the financial support by Deutsche Forschungsgemeinschaft and by Verein der Freunde und Förderer der Universität zu Köln.

References

[1] Cargill G S III 1970 *J. Appl. Phys.* **41** 12
[2] Albert K, Kovaz Z and Lilienthal H R 1967 *J. Appl. Phys.* **38** 1258
[3] Berrada A, Lapierre M F, Loegel B, Panissod P and Robert C 1978 *J. Phys. F: Met. Phys.* **8** 845
[4] Hüller K, Dietz G, Hausmann R and Kölpin K 1985 *J. Magn. Magn. Mater.* **53** 103
[5] Sonnberger R, Pfanner E and Dietz G 1986 *Z. Phys.* B **63** 203
[6] Dietz G, Laska T, Schneider H D and Stein F 1988 *J. Less-Common Met.* **145** 573
[7] Sonnberger R and Dietz G 1987 *Z. Phys.* B **66** 459
[8] Bakonyi I, Varga L K, Lovas A, Toth-Kàdár E and Sólyom A 1985 *J. Magn. Magn. Mater.* **50** 111
[9] Stoner E C 1940 *Proc. Phys. Soc.* **52** 175
[10] Stoner E C and Wohlfarth E P 1948 *Phil. Trans. R. Soc.* **240** 599
[11] Néel L 1947 *C.R. Acad. Sci. Paris* **224** 1550
[12] Brenner A 1963 *Electrodeposition of Alloys* (New York: Academic)
[13] Néel L 1953 *Rev. Mod. Phys.* **25** 293
[14] Brown W F 1959 *J. Appl. Phys.* **30** *Suppl.* 130S
[15] Kittel C 1946 *Phys. Rev.* **70** 965; 1949 *Rev. Mod. Phys.* **21** 541
[16] Frei E H, Strikman S and Treves D 1957 *Phys. Rev.* **106** 446
[17] Kneller E 1962 *Ferromagnetismus* (Berlin: Springer) p 432
[18] Gibbs M R J and Evetts J E 1980 *Scr. Metall.* **14** 63
[19] Primak W 1955 *Phys. Rev.* **100** 1677